

*Galaxy Dynamics: from the Early Universe to the Present*  
*ASP Conference Series, Vol. 197, 2000*  
*F. Combes, G. A. Mamon and V. Charmandaris, eds., p. 367*

## Theory of galaxy dynamics in clusters and groups

Gary A. Mamon

*Institut d’Astrophysique, F-75014 Paris, FRANCE*

**Abstract.** Analytical estimates of the mass and radial dependence of the rates of galaxy mergers and of tidal interactions are derived for clusters and groups of galaxies, taking into account the tides from the system potential that limit the sizes of galaxies. Only high mass galaxies undergo significant major merging before being themselves cannibalized by more massive galaxies. Strong tides from the group/cluster potential severely limit the merger/tide cross-sections in the central regions, and while tides are most efficient at the periphery, one should see merging encounters further inside rich clusters.

### 1. Introduction

Mergers of galaxies in slow collisions and tidal interactions in rapid collisions are two key dynamical processes that occur in groups and clusters of galaxies. Cosmological  $N$ -body simulations are beginning to approach the resolution necessary to study galaxy dynamics in groups and clusters (see Moore, in these proceedings). Moreover, mergers and tidal collisions leave significant observational signatures, in the form of tidal tails, asymmetries and generally disturbed morphologies and internal kinematics (see Amram, in these proceedings). Also, galaxy merging is an essential mechanism for driving elliptical galaxy morphologies given disk-like progenitors. As such, an understanding of galaxy merging is very important for semi-analytical modeling of galaxy formation.

In this review, I compute analytically the rates at which a galaxy of given mass and position within a cluster or group with a Navarro, Frenk, & White (1995, NFW) potential undergoes slow major mergers with lower mass galaxies and rapid tidal encounters. Since the collision cross-sections are strongly modulated by the tides from the group/cluster potential, I begin with a simple formalism for estimating the tides from the system potential. Note that I will not consider ram pressure stripping on galaxies.

### 2. Tides from the cluster/group potential

The potential of a cluster can exert a strong differential force on a galaxy orbiting within it, but these tides are strongly dependent on the galaxy orbit.

A galaxy on a nearly circular orbit is likely to be tidally locked, as the Moon is with respect to the Earth. In this case, the tidal force is simply (King, 1962)

$$F_{\text{tide}} = \Delta \left[ \frac{GM(R)}{R^2} - \Omega^2(R) \right] \quad (1)$$

and equating  $F_{\text{tide}}$  in eq. (1) to the force,  $f = Gm(r)/r^2$  that a galaxy exerts on one of its stars yields for  $r \ll R$  a galaxy tidal radius  $r_t$  that satisfies a velocity modulated density criterion (see Mamon, 1995):

$$\bar{\rho}_g(r_t) = \bar{\rho}_{\text{cl}}(R) \left[ 2 - \frac{3\rho_{\text{cl}}(R)}{\bar{\rho}_{\text{cl}}(R)} + \frac{V_p^2(R)}{V_{\text{circ}}^2(R)} \right] , \quad (2)$$

where  $V_p$  and  $V_{\text{circ}}$  are respectively the galaxy's velocity at pericenter and the cluster's circular velocity. The term in brackets in eq. (2) is 2 for circular orbits. Moreover, for a singular isothermal law  $\rho \sim r^{-2}$  for both galaxy and cluster, one finds (see White, 1983) that for circular orbits the galaxy size is proportional to its clustocentric radius:  $r_t = 2^{-1/2}(v_{\text{circ}}/V_{\text{circ}})R$ , where  $v_{\text{circ}}$  is the circular velocity of the galaxy. For general density profiles, writing  $\bar{\rho}(r) \sim v_{\text{circ}}^2(r)/r^2$ , one obtains

$$\frac{r_t/R}{v_{\text{circ}}(r_t)/V_{\text{circ}}(R)} = \left( 2 - 3 \frac{\rho}{\bar{\rho}} + V_p^2/V_{\text{circ}}^2(R) \right)^{-1/2} . \quad (3)$$

Merritt (1984) used a similar circular-tide criterion to argue that galaxies are strongly tidally limited by the cluster potential.

However, cosmological infall imposes elongated orbits. A galaxy on an elongated orbit experiences a strong tide during its rapid, hence short, passage at pericenter, prompting Ostriker, Spitzer, & Chevalier (1972) to introduce the term *tidal shock*. During this shock, a star in the galaxy experiences a velocity impulse

$$\Delta v \sim F_{\text{tide}} \Delta t \sim \frac{GM(R_p) r}{R_p^3} \left( \frac{R_p}{V_p} \right) = \text{cst} \frac{GM(R_p) r}{R_p^2 V_p} , \quad (4)$$

where we neglected the centrifugal term in  $F_{\text{tide}}$ , because the galaxy falls in too fast to be phase locked. A more precise calculation by Spitzer (1958), who introduced the *impulsive approximation* where the point-mass perturber moves at constant  $\mathbf{V}$ , produces the same relation as in eq. (4) with a constant of order unity. The impulse approximation can also be applied to extended perturbers (Aguilar & White, 1995; Mamon, 1987). Recently, Gnedin, Hernquist, & Ostriker (1999) applied the impulsive approximation to the more realistic Hernquist (1990) potential and found a dependence of  $\Delta v$  matching that of eq. (4), with a very small dependence on  $R_p$  and again the constant is found to be of order unity for elongated orbits (with order of unity changes when they performed orbit-integrated — instead of straight-line — tidal calculations).

The tidal radius can then be defined as that where the energy increment caused by the tidal perturbation is equal to the binding energy (White, 1983).

With  $E \sim Gm(r_t)/r_t$  and  $\Delta E \sim (\Delta v)^2/2$ , one obtains another velocity modulated density criterion

$$\bar{\rho}_g(r_t) \simeq \bar{\rho}_{\text{cl}}(R_p) \left( \frac{V_{\text{circ}}(R_p)}{V_p} \right)^2, \quad (5)$$

which for any density profile yields

$$\frac{r_t/R}{v_{\text{circ}}(r_t)/V_{\text{circ}}(R)} = \frac{V_p}{V_{\text{circ}}}. \quad (6)$$

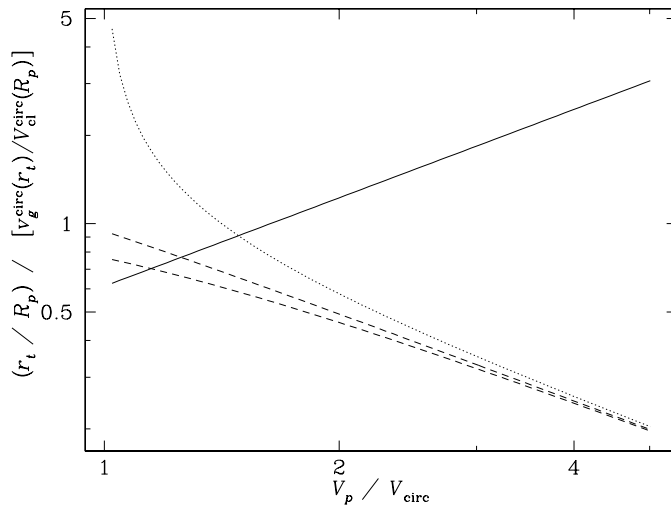


Figure 1. Velocity modulation of normalized tidal radii for given orbit pericenter. The *solid curve* shows impulsive tides for elongated orbits (eq. [6]). The *dashed curves* show circular tides (eq. [3]) in a Navarro, Frenk, & White potential for 0.1 (*upper curve*) and 1 (*lower curve*) scale radii. The *dotted curve* shows the circular tide within a homogeneous core.

Figure 1 shows the effects of velocity modulation on the tidal radii. The effective tidal radius should be taken as the largest of the circular and impulsive regimes (otherwise one would be left with discontinuities in the transition  $V_p$  from near-circular to elongated orbits). Hence, with homogeneous cores, circular tidal theory produces increasingly smaller tidal radii for orbits of increasing but low elongation, as Merritt & White (1987) found in their  $N$ -body simulations. With cuspy cores as in the NFW profile, low-elongation non-circular orbits experience tidal shocks instead. The orbit elongation,  $R_p/R_a \simeq 0.2$ , found in Ghigna et al.'s (1998) high-resolution cosmological simulations corresponds to  $V_p/V_{\text{circ}}(R_p) \simeq 1.5 - 2.7$ , roughly yielding

$$r_t \simeq (1.2 - 1.5) R_p \left( \frac{v_{\text{circ}}}{V_{\text{circ}}} \right) \approx (1.2 - 1.5) R_p \left( \frac{v_g}{v_{\text{cl}}} \right) \quad (7)$$

as for singular isothermal models, where  $v_g$  and  $v_{\text{cl}}$  are the mean galaxy and cluster velocity dispersions, respectively. If  $V_p \simeq V_{\text{circ}}(R_p)$  and if galaxy and cluster density profiles are self-similar, then tides from the cluster potential would force the simple relation  $m(r_t)/m(r_{\text{vir}}) = M(R_p)/M(R_{\text{vir}})$ . In fact, using  $V_p/V_{\text{circ}}(R_p)$  expected for the NFW profile, assuming  $\langle R \rangle \simeq 4R_p$ , and adopting the departures from self-similarity in the NFW profiles noted by Navarro, Frenk, & White (1997, lower mass NFW profiles are more centrally concentrated), one finds

$$\frac{m(r_t)}{m(r_{\text{vir}})} \simeq \left[ \frac{M(R)}{M(R_{\text{vir}})} \right]^{b_m} \simeq a_r \left( \frac{R}{R_{\text{vir}}} \right)^{b_r}, \quad (8)$$

where for clusters ( $v_{\text{cl}} = 1000 \text{ km s}^{-1}$ ) and groups ( $v_{\text{cl}} = 300 \text{ km s}^{-1}$ ) we respectively have  $b_m = 0.50$  and  $0.82$ ,  $a_r = 0.58$  and  $0.52$ , and  $b_r = 0.57$  and  $0.78$  (eq. [8] is accurate to better than 5% for  $R > 0.05 R_{\text{vir}}$ ).

### 3. Galaxy merger rates in clusters and groups

#### 3.1. Global merger rates for equal mass galaxies

The rate of mergers is obtained by integrating over velocities the merger cross-sections:

$$k \equiv \frac{1}{n^2} \frac{d^2N}{dt dV} = \langle vs(v) \rangle = \int_0^\infty dv f(v) vs(v), \quad (9)$$

where  $s(v) = \pi[p_{\text{crit}}(v)]^2$  is the merger cross-section and  $f(v)$  is the distribution of relative velocities (with  $\int_0^\infty f(v) dv = 1$ ). Hence,  $nk \equiv dN/dt$  is the rate at which a galaxy suffers a merger. Within the virialized regions of clusters with 1D velocity dispersion  $v_{\text{cl}}$ , the velocity distribution is a gaussian with standard deviation  $2^{-1/2}v_{\text{cl}}$ :  $f(v) = 2^{-1}\pi^{-1/2}v_{\text{cl}}^{-3}v^2 \exp[-v^2/(4v_{\text{cl}}^2)]$ .

Roos & Norman (1979), Aarseth & Fall (1980) and Farouki & Shapiro (1982) have established merger cross-sections from very small  $N$ -body simulations of galaxy collisions, that were based upon the parameters at closest approach. The maximum distance of closest approach,  $r_p^{\text{max}}$ , was 4 (Aarseth & Fall) or 11 (Farouki & Shapiro) times the mean galaxy half-mass radius,  $r_h$ . Mamon (1992) used the Roos & Norman cross-section with the Aarseth & Fall scaling to derive a merger rate.

However, the gaussian approximation for the relative velocity distribution implies that the cross-sections used in eq. (9) are based upon impact parameters (at infinity) and not at closest approach. Makino & Hut (1997) derived merger cross-sections using high resolution  $N$ -body simulations of colliding galaxies with more realistic density profiles. Their cross-sections are expressed in terms of impact parameters.

Kravitsky & Kontorovich (1997) used a simple gravitational focusing recipe to connect the cross-section at closest approach (which they assumed to be independent of pericentric velocity), in units of the velocity at infinity, to the cross-section at infinity (without making any assumption on the potential energy of interaction of the colliding pair). Note that Makino & Hut show that  $r_p^{\text{max}} > 10 r_h$ , while Kravitsky & Kontorovich argue that it is approximately the sum of the galaxy *radii* (which are ill-defined).

Figure 2 shows the dimensionless merger rates  $k/(r_h^2 v_g)$ , where  $v_g$  is the mean galaxy internal velocity dispersion, derived from Mamon (1992), Makino & Hut (1997), and Krivitsky & Kontorovich (1997). I rescale the rates of Krivitsky & Kontorovich in terms of half-mass radii using  $R = 9 r_h$  (to obtain merger rates similar to those of Makino & Hut), *i.e.*,  $r_p^{\max}/r_h = 18$ .

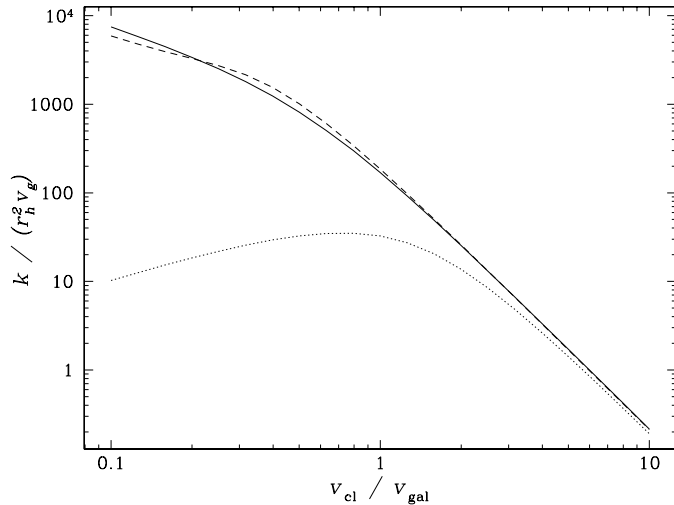


Figure 2. Dimensionless merger rates  $k/(r_h^2 v_g)$  (see eq. [9]) as a function of the ratio of cluster to galaxy velocity dispersion. The *dotted*, *solid* and *dashed* curves respectively correspond to the rates of Mamon (1992), Makino & Hut (1997, using Hernquist, 1990 model galaxies) and Krivitsky & Kontorovich (1997, rescaled vertically, because they reason in terms of galaxy radii rather than galaxy half-mass radii).

The agreement between the merger rates of Krivitsky & Kontorovich and Makino & Hut is remarkable, given the very simple analytical formulation of the former authors (but again this required a rescaling, or, in other words, a choice of  $r_p^{\max}/r_h = 18$ ). The very low merger rate of Mamon (1992) in the group regime ( $v_{\text{cl}} \approx v_g$ ) is a consequence of the lack of gravitational focusing in that model.

The merger rates of Mamon (1992) and Makino & Hut agree to within 15% in the cluster regime ( $v_{\text{cl}} \gtrsim 4 v_g$ ). This agreement is almost fortuitous since Mamon shows that the merger rate with the Roos & Norman cross-section scales as  $(r_p^{\max}/r_h)^2$ , while this ratio is very different in Makino & Hut's cross-section. In any event, in the cluster regime the merger rate can then be written

$$k = b \frac{r_h^2 v_g^4}{v_{\text{cl}}^3} = a \frac{G^2 m^2}{v_{\text{cl}}^3}, \quad (10)$$

where  $a \simeq 8$  (Mamon, 1992). With  $3 v_g^2 \simeq 0.4 Gm/r_h$  (Spitzer, 1969), appropriate for the Hernquist model, the Makino & Hut rate translates to  $a = 12$ . Figure 2 shows that  $k \sim v_{\text{cl}}^{-3}$ , whichever merger cross-section is used. In fact,

it is easy to show that *for any merger cross-section rapidly decreasing with increasing velocity*, the merger rate should scale as  $v_{\text{cl}}^{-3}$  for  $v_{\text{cl}} \gg v_g$ , as first found by Mamon (1992) for the Roos & Norman cross-section.

The important conclusion of Figure 2 is that *for given galaxy parameters, the merger rate is roughly 100 times lower in rich clusters than in poor groups of galaxies*.

### 3.2. Merger rates for different masses

If the critical merging velocity  $v_{\text{crit}}$  is a function of  $r_p/r_h$  (Aarseth & Fall, 1980; Farouki & Shapiro, 1982), it is easy to show that  $k \sim r_h^2$ , and if  $v_{\text{crit}}$  is a function of  $r_p/\langle r_h \rangle$ , then  $k \sim \langle r_h \rangle^2$  (see Mamon, 1992). Similarly, it is reasonable to expect that  $k \sim \langle v_g^2 \rangle^2$ . Then, given eq. (10) and that  $m \sim r_h^3$ , the rate of mergers of a galaxy of mass  $m$  with a galaxy of mass  $\lambda m$

$$k(m, \lambda m) = \frac{aG^2 m^2}{v_{\text{cl}}^3} \left( \frac{1 + \lambda^{1/3}}{2} \right)^2 \left( \frac{1 + \lambda^{2/3}}{2} \right)^2. \quad (11)$$

A given galaxy undergoes mergers with other galaxies at a rate

$$\mathcal{R} \equiv n\bar{k}(m) = \int_{\lambda_{\min}}^{\lambda_{\max}} k(m, \lambda m) n(\lambda m) d(\lambda m), \quad (12)$$

where for major mergers with smaller galaxies (that transform disk galaxies into ellipticals),  $\lambda_{\min} \simeq 1/3$  and  $\lambda_{\max} = 1$ , while for destruction by mergers with larger galaxies,  $\lambda_{\min} = 1$  and  $\lambda_{\max} \rightarrow \infty$ . Adopting a Schechter (1976) form for the mass function of galaxies,  $n(m) = (n_*/m_*) x^{-\alpha} \exp(-x)$ , where  $x = m/m_*$ , eqs. (11) and (12) yield

$$\mathcal{R} = n\bar{k} = \frac{aG^2 n_* m_*^2}{16 v_{\text{cl}}^3} K(m/m_*), \quad (13)$$

$$K_{\text{major}}(x) = x^{3-\alpha} \sum_{j=0}^6 \text{Min}(j, 7-j) [\Gamma(1+j/3-\alpha, x/3) - \Gamma(1+j/3-\alpha, x)], \quad (14)$$

$$K_{\text{destr}}(x) = x^{3-\alpha} \sum_{j=0}^6 \text{Min}(j, 7-j) \Gamma(1+j/3-\alpha, x). \quad (15)$$

Figure 3 shows the expected number of major mergers with smaller galaxies and destruction by mergers with larger galaxies that a galaxy of a given mass should expect in a Hubble time if it sits in a typical location of a rich cluster, assuming a constant rate in time. The rise in merger rates at low mass reflects the rise of merger cross-section with mass, while the decrease at high mass is caused by the sharp decrease in the galaxy mass function yielding few galaxies to merge with. Figure 3 clearly indicates that *the probability of merger for a given galaxy is always small*. Moreover, *low and intermediate mass galaxies ( $m < m_*$ ) are usually cannibalized before undergoing major mergers*.

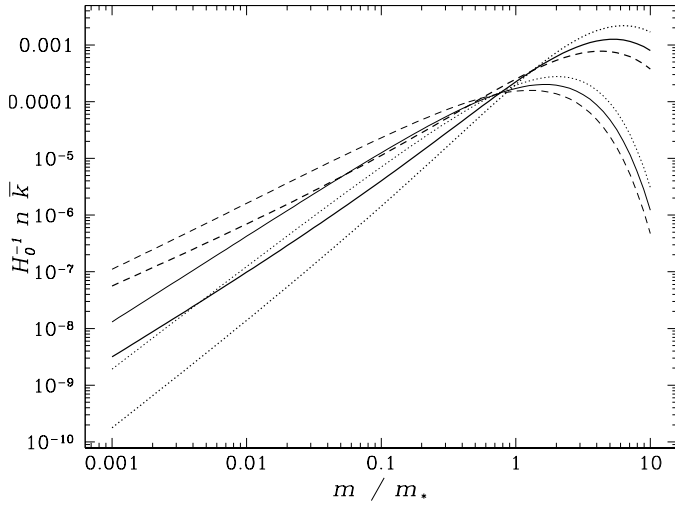


Figure 3. Number of major mergers with lower mass galaxies (eqs. [13] and [14], *thick curves*) and higher mass galaxies (eqs. [13] and [15], *thin curves*) extrapolated to one Hubble time versus galaxy mass. *Dotted, solid and dashed curves* are for  $\alpha = -1.1, -1.3$  and  $-1.5$ , respectively. The normalization assumes  $a = 12$ ,  $v_{\text{cl}} = 1000 \text{ km s}^{-1}$ ,  $n_* = 200 n_*^{\text{field}}$ , with  $n_*^{\text{field}} = 0.013 h^3 \text{ Mpc}^{-3}$  (Marzke et al., 1998), and  $m_* = 0.1 (M/L)_{\text{cl}} \ell_* = 3 \times 10^{11} h^{-1} M_\odot$ .

### 3.3. Variation of merger rates with position in cluster

One can go one step further and predict the variation of the merger rate with position in the cluster. From eq. (13), the merger rate scales with radius as

$$\mathcal{R}(R, m) = \frac{a G^2 m_* \mu^2(R) \rho_{\text{cl}}(R)}{16 \Gamma(2-\alpha, x_m) v_{\text{cl}}^3(R)} K(m/m_*) , \quad (16)$$

where  $\mu(R) = m(r_t)/m(r_{\text{vir}})$  (see eq. [8]),  $m_*$  is the mass at the break of the *field* galaxy mass function and  $x_m$  is the minimum galaxy mass in units of  $m_*$ .

Assuming a mass density profile  $\rho \sim R^{-\beta}$  and arguing that cluster galaxies are severely tidally truncated by the cluster potential as  $r_{\text{gal}} \sim R$  (i.e. with eq. [7] and assuming constant  $R_p/R_a$ ), Mamon (1992) showed that if galaxies also follow the law  $\rho \sim r^{-\beta}$ , then their masses obey  $m \sim R^{3-\beta}$ . Note that this sharp scaling of galaxy size with clustocentric distance is now confirmed in high resolution cosmological simulations of clusters (Ghigna et al., 1998). Hence, *the radial variation of merger rates are strongly modulated by potential tides*.

By writing  $n(R) \sim \rho(R)/m(R) \sim R^{-3}$ , I derived  $nk \sim R^{-\beta/2}$ , hence a higher merger rate inside the cluster, with a slope agreeing perfectly with the observed elliptical fraction (Whitmore, Gilmore, & Jones, 1993), given  $\beta = 9/4$  as predicted in early models of cluster formation (Bertschinger, 1985). The derivation above has one flaw: although galaxy masses were correctly scaled to increase with  $R$ , I forgot to scale the fraction of cluster mass lying within

galaxies in the same way. Therefore, one really expects  $n(R) \sim \rho(R) \sim R^{-\beta}$  and  $nk \sim R^{3-3\beta/2}$  yielding a slope  $d \ln(nk) / d \ln R = -3/8$  for  $\beta = 9/4$  and a null slope for  $\beta = 2$ , both in disagreement with the logarithmic gradient of elliptical fraction found by Whitmore et al..

One can use the more realistic NFW density profiles to estimate the radial dependence of the merger rates. An essential parameter is  $\langle R_p/R \rangle$ , which measures the effectiveness of the tides from the cluster potential. Because the dynamical friction time scales as  $M/m$  times the orbital time (Mamon, 1995), orbit circularization, which to first order operates on a dynamical friction time scale, should be very slow for galaxies falling onto clusters, but fairly effective for galaxies falling into small groups.

Figure 4 shows the predicted number of major mergers in rich clusters and small groups, extrapolated over a Hubble time, using the non-self-similarity of the NFW profiles, an exact scaling of the typical galaxy mass  $m_*$  with radius (see eq. [8]), and partial orbit circularization in groups.

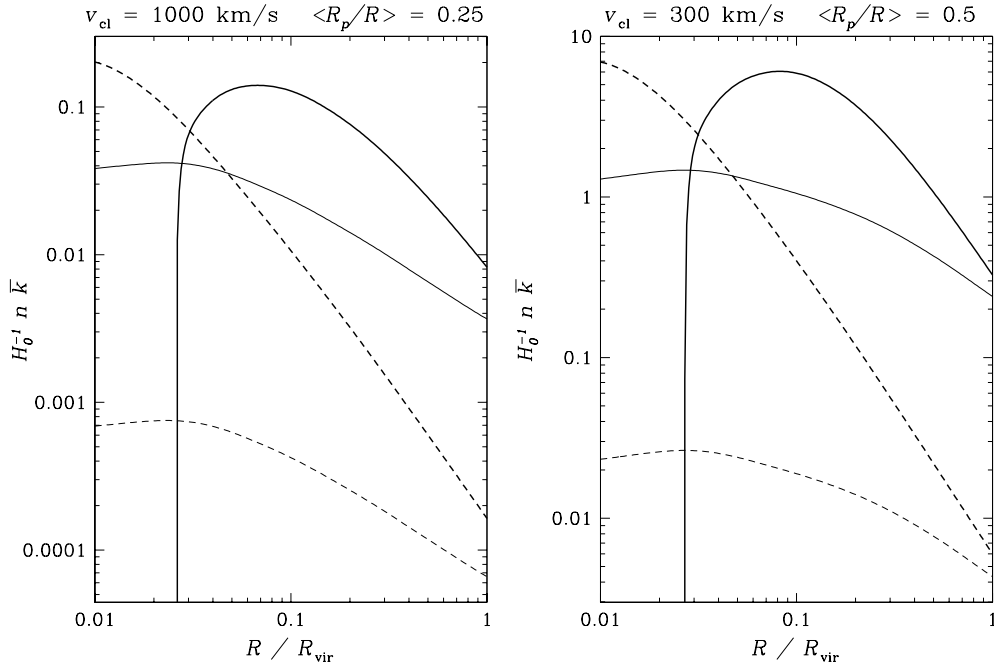


Figure 4. Number of major mergers a given galaxy undergoes with lower mass galaxies (eq. [16], with eqs. [13] and [14]), extrapolated to one Hubble time, versus clustocentric radius in (left) an NFW cluster with  $v_{\text{cl}} = 1000 \text{ km s}^{-1}$  and (right) a group with  $v_{\text{cl}} = 300 \text{ km s}^{-1}$ , where the galaxy mass function has  $\alpha = 1.3$ . The *solid thick* and *dashed thick* curves represent the expected number of major mergers for galaxies of mass  $m = m_*^{\text{field}} = \Omega_0 \rho_c / [n_*^{\text{field}} \Gamma(2 - \alpha, x_m)] = 5 \times 10^{12} h^{-1} M_\odot$  and  $m = 0.1 m_*^{\text{field}} = 5 \times 10^{11} h^{-1} M_\odot$ , respectively. The *solid thin* and *dashed thin* curves refer to galaxy masses  $m = m_*(R)$  and  $m = 0.1 m_*(R)$ , respectively.

The merger rates for constant mass galaxies fall off sharply at small clustocentric radii, simply because tidal truncation of galaxies is so severe that there are no galaxies left that are massive enough to produce a major merger with our test galaxy. In general, the merger rates are maximum for intermediate radii for given test galaxy masses, and at low radii for fixed  $m/m_*(R)$  (recall though that low mass galaxies get cannibalized before they can undergo a major merger with a smaller galaxy). In any event, Figure 4 confirms that *mergers are ineffective in clusters, but very effective in small groups*. Note that without resorting to partial orbit circularization within groups, the expected number of mergers in groups is somewhat less than expected from the  $v_{\text{cl}}^{-3}$  scaling, because, relative to clusters, the more concentrated NFW profiles in groups lead to stronger modulation of the merger rate by the potential tides.

#### 4. Collisional tidal stripping in clusters and groups

Because non-merging galaxy collisions are by essence rapid, they can be treated as tidal shocks, and it is reasonable to assume that for tidal features to be visible, one requires  $\Delta E \geq \gamma |E|$ , where  $\gamma \lesssim 1$ . Hence,  $\Delta v \geq (3\gamma)^{1/2} v_g$ . Denoting  $p$  and  $V$  the separation and relative velocity at pericenter, and  $v_{\text{circ},p}(p)$  the circular velocity of the perturbing galaxy out to  $p$ , eq. (4) leads to a critical impact parameter

$$p_{\text{crit}} = \frac{r}{(3\gamma)^{1/2}} \frac{v_{\text{circ},p}^2}{v_g V} , \quad (17)$$

where we note that  $v_{\text{circ},p}$  is almost independent of  $p$  for realistic density profiles for the perturbing galaxy. Then, integrating the cross-sections derived from eq. (17), the rate of tidal interactions is

$$k = \langle vs(v) \rangle = \frac{\pi^{1/2}}{3\gamma} \left( \frac{r}{v_g} \right)^2 \frac{v_{\text{circ},p}^4}{v_{\text{cl}}} , \quad (18)$$

and is virtually independent of the test galaxy parameters. Integrating eq. (18) over perturber mass and remarking that both the galaxy and the perturbers are tidally limited by the cluster potential, one obtains using eq. (5)

$$n \bar{k} = \frac{\Gamma(7/3 - \alpha, x_m)}{4\pi^{1/2} \gamma G \Gamma(2 - \alpha, x_m)} \left( \frac{v_{\text{circ}}}{v_g} \right)^2 \frac{v_{\text{circ},*}^4}{m_*} \frac{\rho_{\text{cl}}(R) \mu^{7/3}(R)}{\bar{\rho}_{\text{cl}}(R_p) v_{\text{cl}}(R)} \left[ \frac{V_p}{V_{\text{circ}}(R_p)} \right]^2 , \quad (19)$$

where again  $\mu(R) = m(r_t)/m(r_{\text{vir}})$  (see eq. [8]),  $v_{\text{circ},*}$  is the circular velocity at the virial radius for a field  $m_*$  galaxy. Again, *the rate of tidal encounters is independent of the galaxy mass*. Note that the  $\mu^{7/3}(R)$  dependence of the rate of tidal encounters illustrates the strong modulation of this rate by the tides from the cluster potential.

Figure 5 shows the expected (eq. [19]) number of strong tidal collisions for galaxies in clusters and groups, with  $\langle R/R_p \rangle$  as in Figure 4. Although groups are preferential sites for strong tidal encounters, galaxies in the outskirts of clusters should also witness such interactions. However, the signature of tidal interactions lasts of order  $1 h^{-1}$  Gyr, so that the fraction of galaxies in clusters

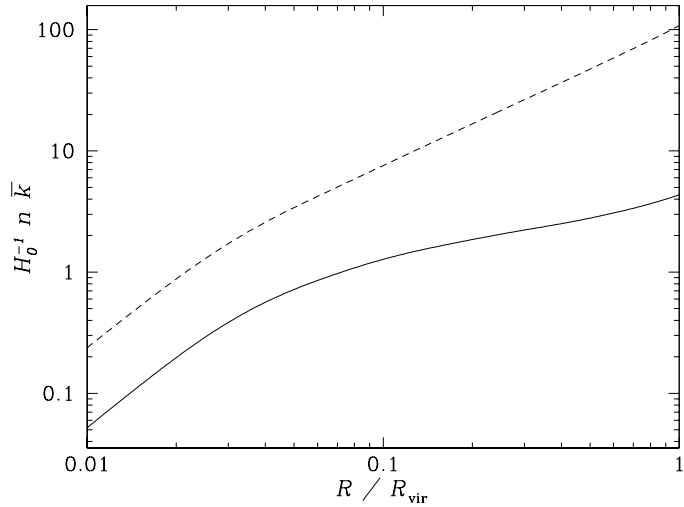


Figure 5. Number of strong ( $\gamma = 1/3$ ) tidal encounters a given galaxy undergoes (eq. [19]), extrapolated to one Hubble time, versus clustocentric radius in an NFW cluster with  $v_{\text{cl}} = 1000 \text{ km s}^{-1}$  (solid curve) and a group with  $v_{\text{cl}} = 300 \text{ km s}^{-1}$  (dashed curve). The galaxy mass function has  $\alpha = 1.3$  with field  $m_* = 5 \times 10^{12} h^{-1} M_\odot$ .

and groups that are currently undergoing tidal interactions is roughly one-tenth of what is displayed in Figure 5.

## 5. Discussion

The strong radial dependence of galaxy masses, predicted by the tidal theory (eq. 8), is clear in the cosmological simulations of Ghigna et al. (1998). Should we then witness *inverse luminosity segregation* in clusters where, outside of the core, galaxies become more luminous towards the cluster periphery? Indeed, Adami, Biviano, & Mazure (1998) found a weak trend of mean galaxy magnitude versus radius for an ensemble of clusters, although they worry that this trend is caused by observational bias. It may be that incompleteness of the observational samples is washing out the trend rather than creating it.

The lack of mergers in present-day rich clusters has been noted in cosmological simulations of clusters (Ghigna et al., 1998). Figure 4 shows that in rich clusters, mergers are at best marginally probable for high mass galaxies lying in the cluster body. Given that high mass galaxies are rare, such merging will be difficult (but not impossible) to detect observationally or in simulations.

From their H $\alpha$  prism surveys of galaxies in clusters, Moss and co-workers (Moss & Whittle, 1993; Moss, Whittle, & Pesce, 1998; Bennett & Moss, 1998) note  $\simeq 30\%$  of spiral galaxies in rich clusters exhibit a *compact H $\alpha$*  morphology and roughly half of these tend to be morphologically disturbed *and* have nearby neighbors. Another half of these compact H $\alpha$  emission galaxies are in the cluster

core, and presumably those have no tidal companions, suggesting that they are harassed by the cluster potential. But the first half, outside the core are probably *bona fide* cases of strong tidal interactions within clusters, leading to an overall frequency of 20% of all galaxies outside the cores of clusters. It remains to be seen if they are associated to substructures such as infalling groups. Correcting Figure 5 for the 1 Gyr duration of these tidal features produces an absolute frequency of tidally interacting galaxies in clusters in rough agreement with that found by Moss and co-workers.

## References

Aarseth, S. J., & Fall, S. M. 1980, ApJ, 236, 43

Adami, C., Biviano, A., & Mazure, A. 1998, A&A, 331, 439

Aguilar, L. A., & White, S. D. M. 1985, ApJ, 295, 374

Bennett, S. M., & Moss, C. 1998, A&AS, 132, 55

Bertschinger, E. 1985, ApJS, 58, 39

Farouki, R. T., & Shapiro, S. L. 1982, ApJ, 259, 103

Ghigna, S., Moore, B., Governato, F., Lake, G., Quinn, T., & Stadel, J. 1998, MNRAS, 300, 146

Gnedin, O. Y., Hernquist, L., & Ostriker, J. P. 1999, ApJ, 514, 109

Hernquist, L. 1990, ApJ, 356, 359

King, I. 1962, AJ, 67, 471

Kravitsky, D. S., & Kontorovich, V. M. 1997, A&A, 327, 921

Makino, J., & Hut, P. 1997, ApJ, 481, 83

Mamon, G. A. 1987, ApJ, 321, 622

Mamon, G. A. 1992, ApJ, 401, L3

Mamon, G. A. 1995, in 3rd Paris cosmology colloq., ed. H. de Vega, & N., Sánchez (Singapore: World Scientific), 95, astro-ph/9511101

Marzke, R. O., da Costa, L. N., Pellegrini, P. S., Willmer, C. N. A., & Geller, M. J. 1998, ApJ, 503, 617

Merritt, D. 1984, ApJ, 276, 26

Merritt, D., & White, S. D. M. 1987, in IAU Symp. 117, Dark Matter in the Universe, ed. J. Kormendy & G. R. Knapp (Dordrecht: Reidel), 283

Moss, C., & Whittle, M. 1993, ApJ, 407, L17

Moss, C., Whittle, M., & Pesce, J. E. 1998, MNRAS, 300, 205

Navarro, J. F., Frenk, C. S., & White, S. D. M. 1995, MNRAS, 275, 720

Navarro, J. F., Frenk, C. S., & White, S. D. M. 1997, ApJ, 490, 493

Ostriker, J. P., Spitzer, L., & Chevalier, R. A. 1972, ApJ, 176, L51

Roos, N., & Norman, C. A. 1979, A&A, 76, 75

Schechter, P. 1976, ApJ, 203, 297

Spitzer, L. 1958, ApJ, 127, 17

Spitzer, L. 1969, ApJ, 158, L139

White, S. D. M. 1983, in Morphology and Dynamics of Galaxies, ed. L. Martinet & M. Mayor (Sauverny: Geneva Obs.), 289

Whitmore, B. C., Gilmore, D. M., & Jones, C. 1993, ApJ, 407, 489